EARTHQUAKE ENGINEERING AND STRUCTURAL DYNAMICS
Earthquake Engng Struct. Dyn. (2016)
Published online XX in Wiley InterScience-(www.interscience.wiley.com). DOI: XX

SITE DEPENDENCE AND RECORD SELECTION SCHEMES FOR BUILDING FRAGILITY AND REGIONAL LOSS ASSESSMENT

Mohsen Kohrangi[1*†], Dimitrios Vamvatsikos[2] and Paolo Bazzurro[3]

[1] *Research assistant, University School of Advanced Studies IUSS Pavia, Pavia, Italy*
[2] *Assistant Professor, School of Civil Engineering, National Technical University of Athens, Greece*
[3] *Professor, University School of Advanced Studies IUSS Pavia, Pavia, Italy*

SUMMARY

When performing loss assessment of a geographically dispersed building portfolio, the response or loss (fragility or vulnerability) function of any given archetype building is typically considered to be a consistent property of the building itself. On the other hand, recent advances in record selection have shown that the seismic response of a structure is, in general, dependent on the nature of the hazard at the site of interest. This apparent contradiction begs the question: Are building fragility and vulnerability functions independent of site, and if not, what can be done to avoid having to reassess them for each site of interest? In the following, we show that there is a non-negligible influence of the site, the degree of which depends on the intensity measure adopted for assessment. Employing a single-period (e.g., first-mode) spectral acceleration would require careful record selection at each site and result to significant site-to-site variability of the fragility or vulnerability function. On the other hand, an intensity measure comprising the geometric mean of multiple spectral accelerations considerably reduces such variability. In tandem with a conditional spectrum record selection that accounts for multiple sites, it can offer a viable approach for incorporating the effect of site-dependence into fragility and vulnerability estimates.

KEY WORDS: Regional loss assessment; building response site-dependence; record selection; conditional spectrum

1. INTRODUCTION

Fragility and vulnerability functions play a central role in both building-specific and regional loss assessment in earthquake engineering. Formally, a building-fragility function can be broadly defined as a probability-valued function of the seismic intensity measure (IM), conveying the probability of violating (or “exceeding”) a certain limit-state (or set of

[*] Correspondence to: Mohsen Kohrangi, University School of Advanced Studies IUSS Pavia, Pavia, Italy – IUSS Palazzo del Broletto - Piazza della Vittoria 15, 27100 Pavia, Italy

[†] E-mail: mohsen.kohrangi@gmail.com

consequences) for an entire building. Conversely, a vulnerability function can be defined as a loss-valued function of the seismic intensity measure, offering a statistic (e.g., mean, standard deviation, $16^{th}/50^{th}/84^{th}$ percentile) of the distribution of seismic loss for the building. Strictly speaking, a single vulnerability function is not enough to describe the full distribution of building loss given the IM. For purposes of subsequent discussion, we will adopt the typical convention and loosely use the term in its singular form to imply any and all the needed vulnerability curves for a comprehensive description of loss given the IM.

Four main approaches have evolved for the estimation of fragility and vulnerability functions, comprising 1) empirical, 2) analytical, 3) engineering judgment, and 4) hybrid methods. In empirical methods, data on the actual structural damages observed at building sites after an earthquake are collected and used for generating the vulnerability/fragility functions [1-9]. Assuming that enough data are available and that the ground motion experienced by the damaged buildings can be estimated with a reasonable accuracy, this is perhaps the most reliable of all approaches. When this is not the case, it is often necessary to use numerical analyses in the so-called analytical method, utilizing structural modeling and computer-intensive calculations [10-21] to analyze the losses in a number of representative archetype [22] or index [23] buildings. Judgment-based methods collect data based on the opinion and experience of a group of experts regarding the damage of different types of structures (e.g. ATC-13 [24] and [25]). A combination of any two of the other three methods or of all three is employed in hybrid approaches [26-30].

In applying analytical methods, which by and large are the most used in practice, the engineer generates structural models of different building types adopting either a single-degree-of-freedom (SDoF) or a multi-degree-of-freedom (MDoF) idealization. Then, depending on the desired level of accuracy and simplicity, appropriate structural analysis methods are employed, typically based on either nonlinear static analysis (e.g., capacity-spectrum [17, 31, 32], displacement-based methods [33, 34], etc.) or nonlinear dynamic analysis [19, 21, 35, 36]. In both cases, a major issue is the invariance of a building's (or class-of-buildings') vulnerability/fragility function from the site itself. In other words, it is assumed that conditioning on an appropriate IM, typically the first-mode spectral acceleration SAT_1, or the peak ground acceleration, removes all other traces of the site hazard from a building's response. This issue manifests itself in nonlinear dynamic analysis of the building model employing a suite of records.

When the vulnerability of a portfolio (or class of buildings) that spans multiple sites with different seismic characteristics is of interest, it is common for engineers to adopt one set of records regardless of its consistency with the hazard at any of the portfolio sites to perform Incremental Dynamic Analysis [37] or some form of multi-stripe or cloud analysis (see [38] for their definitions). This procedure results in identical estimates of the distribution of response for given levels of the IM for any archetype building located at different sites. Although less obvious, the same issue is also present in nonlinear static approaches, hidden within the regression functions (and the record suites used for their generation) employed to approximate the equivalent inelastic SDoF dynamic response.

In general, there is significant consensus nowadays that structural response, characterized by any number of engineering demand parameters (EDPs), as well as the corresponding loss conditioned on the IM are not only dependent on the building's characteristics, but also on the hazard conditions at the site where the building is located. Hence, following these thoughts identical buildings should be characterized by different vulnerability functions at two different sites since the magnitude of the earthquakes around the site, the distance to the causative faults nearby the site, the soil type at the building location, etc. can all alter the "signature" of

DOI: XX

the ground motions expected at the site and, therefore, the building response and consequently the predicted damages at the same level of ground motion IM. This is the premise of record selection that has recently risen to challenge the idea that conditioning on a simple IM, such as SAT_1, removes all other traces of the site hazard from a building's EDP response, a desirable property also known as IM sufficiency [39]. In fact, sophisticated schemes have been proposed to minimize such response prediction bias (i.e., to correct any IM insufficiency) by performing building- and site-specific record selection, most notably the Conditional Mean Spectrum (CMS) [40], the Conditional Spectrum (CS) [41] and the Generalized Conditional Intensity Measure (GCIM) [42] approaches.

The implications of site-dependence for seismic response and loss assessment, however, cannot be discounted. This means that the record suite selected to incorporate the seismic hazard of the site into the building seismic response should be representative of the characteristics of that specific site. In addition, in a portfolio analysis, different classes of buildings (e.g., steel, reinforced concrete, masonry) with different properties (height, age, etc.) are typically analyzed. Even establishing the vulnerability functions for a single class of buildings (say, post-Northridge mid-rise steel frames of West USA) typically requires analyzing more than one realization of a single type, more finely differentiating for height, the presence of irregularities, etc. [43]. The record selection, therefore, becomes both building- and site-specific, not to mention IM-level specific, as eminent record-selection approaches [40-42] would generally lead to different record suites for lower versus higher levels of hazard to account for different contributing events.

Although such a rigorous selection process would arguably be the most accurate approach, its implementation in practical applications remains cumbersome. Thus, several attempts have appeared in the literature to address the shortcomings of using a single record suite, although not necessarily all directed at the loss estimation problem. For example, Haselton et al. [35] proposed a simplified method to adjust the IDA estimate of collapse intensity for a set of buildings by accounting for ground motion spectral shape through the concept of "epsilon" (see [44] or Equation 6 for its definition). Rather than modifying estimates of SAT_1 values, as [35] does, other researchers have focused on using more sufficient IMs. Currently, in our opinion the most promising proposal is for employing the averaged spectral acceleration (*AvgSA*), whereby the logarithm of spectral acceleration is averaged over a range of periods [44-48], or other proposals for averaging spectral ordinates in the linear space [49, 50]. Eads et al. [51] used *AvgSA* for assessing the response of a group of 700 buildings with different heights and types, showing that it can be sufficient (i.e., provide a distribution of EDP given the IM that is independent of other ground motion characteristics) and efficient (i.e., provide relatively low dispersion of EDP given the IM) for building collapse risk assessment if an appropriate period range is selected. Aiming instead at capturing the entire range of response that matters for loss estimation, Kazantzi and Vamvatsikos [52] proposed using *AvgSA* as a common, first-mode-period independent IM to assess the vulnerability for a whole class of buildings. They concluded that even without a careful record selection, *AvgSA* offers a prediction of both global and local EDPs for a group of buildings that is substantially improved compared to the prediction based on SAT_1. Going one step further, Kohrangi et al. [53] proposed a record selection method, termed CS(*AvgSA*), that improves upon the *SAT*-based conditional spectrum approach, CS(*SAT*) [41], by changing the conditioning IM from spectral acceleration at a single period to *AvgSA*. Both CS record selection schemes provide suites of records that match the mean and variation of the spectrum, maintaining the hazard consistency *at a single site of interest*. In addition, CS(*AvgSA*) purposefully removes the reliance of CS(*SAT*) on any single period, introducing a number of advantages that will be

DOI: XX

exploited in this study to further incorporate the effect of multiple sites.

Here an alternative, improved record selection approach for portfolio seismic assessment is proposed by re-engineering both CS(*SAT*) and CS(*AvgSA*) to incorporate multi-site effects. It stands on the idea of the “exact” CS method where multiple causal earthquakes and multiple Ground Motion Prediction Equations (GMPEs) are incorporated [54]. As a result, a single set of records is selected to be consistent (to the extent possible) with the hazard at all the sites. This way, even though identical fragility/vulnerability functions are still obtained for identical buildings located at different sites, they are arguably characterized by a fair mean (and perhaps even variability of) response of the buildings at all the sites by systematically considering the inherent site-to-site variability in a single shot. In addition, the CS(*AvgSA*) approach also allows the use of a single scalar IM that can remain common throughout the loss estimation of an entire class of buildings while retaining high sufficiency and efficiency for both peak interstory drifts (IDRs) and peak floor accelerations (PFAs) [52], something impossible to achieve with SAT_1. In the following, the details of the methodologies are presented, together with their application in an illustrative example.

2. PROBLEM DEFINITION

The most accurate way of generating building fragility/vulnerability functions to characterize a group of buildings (either identical ones or similar enough to belong to a single building class according to the taxonomy employed [25]) at multiple sites with different seismic hazard is to derive them separately for each building and site pair. Then, when estimating loss for the building ensemble, one could simply employ the specific functions that characterize each building at a given site and finally aggregate the results. This conceptually “perfect” approach is of little practical appeal, though, as applying it in accordance with our previous discussion would require performing site- and building-specific record selection for several IM levels and using them to run nonlinear dynamic analyses of each structure in question. Furthermore, pairing each building and site to its own fragility/vulnerability function to estimate loss becomes a computer-intensive bookkeeping exercise that requires a wealth of data on the building stock that is often, if not always, unavailable. Thus, the typical state of practice dictates the consideration of a single fragility (per given limit-state) or single vulnerability function for a class of buildings everywhere within the region of interest. The question is how to produce one such fragility/vulnerability function to represent the multiple sites and buildings of a given class, without introducing any bias in the results due to the records selected for its generation.

Let us first focus on a single archetype/index building that is employed at multiple sites as a (full or partial) representation of a class. Similar to what mentioned earlier, in an ideal world, assuming that one has the time and the information, the engineering seismologist could select appropriate records for each site to estimate the fragility/vulnerability on a case-by-case basis. Then, these individual functions could be merged into a single one to represent the statistical characteristics of the entire set, potentially using appropriate weights according to the exposure (i.e., number of such buildings or insured value) at each site. This will be termed the multi-site “multi-run” function as it requires running the analysis of the building multiple times and it obviously carries with it most (if not all) of the problems of the aforementioned “perfect” approach. It will only be used here to serve as a valuable baseline for comparison. To achieve significant practical application potential, we instead wish to account for the multi-site aspect of the problem at a much earlier point, before fragility/vulnerability is estimated, thus gaining true computational savings by running the pertinent response analysis

DOI: XX

only once with a carefully selected single set of accelerograms per IM level. Hence, we aim to integrate the results from multiple sites to select one record suite per IM level that will be used for deriving the so-called multi-site “single-run” fragility or vulnerability function to represent all sites at the same time with a much reduced computational cost.

Note that henceforth our presentation will focus on deriving building fragilities only, yet this is done simply for reasons of convenience. Our results encompass the entirety of the EDP given IM relationship for both drift and acceleration EDPs. Therefore the scope fully includes the estimation of vulnerability as well, even when it is performed (arguably in its most accurate version) via component-based approaches, without recourse to building fragilities per se [20, 55]. Hence, the conclusions to appear remain valid even for the most advanced approaches to account for building vulnerability in loss assessment.

2.1. Definition of a fragility function

In analytical approaches, there are several ways to estimate parameter values for a fragility function that are consistent with the obtained data, depending on the procedure used to evaluate structural response [56]. Fragility functions are commonly defined as lognormal cumulative distribution functions, parameterized by the logarithmic mean θ and logarithmic standard deviation β of the IMs causing exceedance of a specific limit state (LS):

$$\mathrm{P}(\mathrm{LS} \mid IM = x) = \Phi\left(\frac{\ln(\mathrm{x}/\theta)}{\beta}\right) \tag{1}$$

$\mathrm{P}(\mathrm{LS} \mid IM = x)$ is the probability of violating LS given the *IM* being equal to x and $\Phi(\cdot)$ is the standard normal cumulative distribution function. The two main approaches for estimating fragility parameters θ, β from raw data are the method of moments and the method of maximum likelihood. Herein, we use the method of moments for IDA and the method of maximum likelihood for the multi-stripe analysis (MSA). Unlike IDA, when MSA is used and limits on scaling are imposed, the analysis may not be performed up to IM levels where all ground motions exceed the limit-state, especially when close to collapse. This lack of data may render the use of the method of moments practically impossible for some limit-states, while a maximum likelihood approach can still offer useful results.

2.2. One multi-run fragility to rule them all

In general, as the multiple sites are a natural partitioning of the sample space of all sites considered, one can invoke the total probability theorem to state that the probability of exceeding LS on a given building located at n sites over a region is

$$\mathrm{P}(\mathrm{LS} \mid IM) = \sum_{s=1}^{n} P_s \cdot \mathrm{P}(LS \mid IM, s), \tag{2}$$

where $\mathrm{P}(LS \mid IM, s)$ is the fragility of the index building at each site s ($s = 1\ldots n$) comprising the region and P_s the corresponding weight, which depends on the significance of each site and could be defined in proportion to the number of buildings present or, in terms of money, to the replacement cost or to the insured value (i.e., the exposure) at each site. Assuming that $\mathrm{P}(LS \mid IM, s)$ is lognormal with parameters $\theta_{IM,s}$ and $\beta_{IM,s}$, then the corresponding parameters θ_{tot} and β_{tot} of the ensemble fragility can be estimated via an application of the laws of total expectation and total variance [57]:

DOI: XX

$$\theta_{tot} = \exp\left[\sum_{s=1}^{n} P_s \cdot \ln(\theta_{IM,s})\right], \tag{3}$$

$$\beta_{tot} = \sqrt{\sum_{s=1}^{n} P_s \cdot \left[\beta^2_{\ln IM,s} + \left(\ln\left[\frac{\theta_{tot}}{\theta_{IM,s}}\right]\right)^2\right]}. \tag{4}$$

These values will serve as our basis of comparison for the proposed ensemble fragility estimation via CS record-selection.

3. MULTI-SITE CONDITIONAL SPECTRUM RECORD SELECTION

3.1. Original single causal earthquake, single-site approach

A computationally efficient algorithm has been proposed by Jayaram et al. [41] to compute the CS target that considers both the mean and variance of the spectral accelerations at different spectral ordinates for a single site. The procedure for a single scenario is summarized as follows. The conditional mean spectral ordinates at periods T_1 to T_n (i.e., vector of $\{\ln SAT_1,...,\ln SAT_n\}$) conditioned on *IM** is defined as:

$$\mu = \begin{bmatrix} \mu_{\ln SAT_1} + \rho_{\ln SAT_1,\ln IM*} \cdot \varepsilon(IM*) \cdot \sigma_{\ln SAT_1} \\ \mu_{\ln SAT_2} + \rho_{\ln SAT_2,\ln IM*} \cdot \varepsilon(IM*) \cdot \sigma_{\ln SAT_2} \\ \vdots \\ \mu_{\ln SATn} + \rho_{\ln SAT_n,\ln IM*} \cdot \varepsilon(IM*) \cdot \sigma_{\ln SAT_n} \end{bmatrix}, \tag{5}$$

in which μ_{lnSATi} and σ_{lnSATi} are the logarithmic mean and standard deviation of the spectral acceleration at period T_i, obtained from the GMPE for a given scenario (e.g., magnitude, rupture-to-site distance and fault type). $\rho_{\ln SAT2,\ln IM*}$ is the correlation coefficient between the spectral acceleration at period T_i and *IM**. The epsilon value ε(*IM**) is the number of standard deviations by which a given $\ln IM*$ of a recorded ground motion differs from the mean predicted by a GMPE. In general, epsilon can be defined as:

$$\varepsilon(IM) = \frac{\ln IM - \mu_{\ln IM}}{\sigma_{\ln IM}}, \tag{6}$$

where ln*IM* is a given (unscaled) ground motion's recorded value of *IM*. The covariance matrix of the spectral accelerations at multiple ordinates conditioned on *IM** is therefore:

$$\mathbf{\Sigma} = \mathbf{\Sigma}_0 - \frac{1}{\sigma^2_{\ln IM*}} \cdot \mathbf{\Sigma}_1 \cdot \mathbf{\Sigma}_1', \tag{7}$$

where prime denotes transposition of a matrix. $\mathbf{\Sigma_1}$ is defined as

$$\Sigma_1 = \begin{bmatrix} \rho_{\ln SAT_1,\ln IM*} \cdot \sigma_{\ln SAT_1} \cdot \sigma_{\ln IM*} \\ \cdots \\ \rho_{\ln SAT_n,\ln IM*} \cdot \sigma_{\ln SAT_n} \cdot \sigma_{\ln IM*} \end{bmatrix}, \tag{8}$$

$\mathbf{\Sigma_0}$ denotes the (unconditional) covariance matrix of the vector $\{\ln Sa(T_1),...,\ln Sa(T_n)\}$:

DOI: XX

$$\mathbf{\Sigma}_0 = \begin{bmatrix} \sigma^2_{\ln SAT_1} & \cdots & \rho_{\ln SAT_1, \ln SAT_2} \cdot \sigma_{\ln SAT_1} \cdot \sigma_{\ln SAT_n} \\ \vdots & \ddots & \vdots \\ \rho\ (T_n, T_1) \cdot \sigma_{\ln SAT_n} \cdot \sigma_{\ln SAT_1} & \cdots & \sigma^2_{\ln SAT_n} \end{bmatrix}, \tag{9}$$

The diagonal elements of Σ denoted by $\Sigma_{i,i}$ can be expressed as:

$$\Sigma_{i,i} = \sigma^2_{\ln SAT_i} - \frac{1}{\sigma^2_{\ln IM*}} \cdot \rho^2{}_{\ln SAT_i, \ln IM*} \cdot \sigma^2_{\ln SAT_i} \cdot \sigma^2_{\ln IM*}, \tag{10}$$

The standard deviation of SAT_i conditioned on $IM*$ is therefore defined by:

$$\sigma_{\ln SAT_i | \ln IM*} = \ln SAT_i \cdot \sqrt{1 - \rho^2_{\ln SAT_i | \ln IM*}} . \tag{11}$$

3.2. Multiple causal earthquakes, GMPEs and sites: Multi-site single-run approach

Lin et al. [54] proposed a formulation for computing a conditional spectrum incorporating multiple causal earthquakes and GMPEs at a single site. This method is adopted here and extended to incorporate the hazard disaggregation for multiple sites. Such a CS target could be used for selecting a single set of records for analyzing an archetype building at different sites. We can consider the "exact" solution for multiple causal earthquakes, GMPEs and sites weighing all the scenarios (numbered by j), GMPEs (numbered by k), and sites (numbered by s) to estimate the conditional mean and standard deviation of the spectrum:

$$\mu_{\ln SAT_i | \ln IM*} = \sum_s \sum_j \sum_k p_{s,j,k} \cdot \mu_{\ln SAT_i, s, j, k | \ln IM*}, \tag{12}$$

$$\sigma_{\ln SAT_i | \ln IM*} = \sqrt{\sum_s \sum_j \sum_k p_{s,j,k} \cdot \left[\sigma^2_{\ln SAT_i, s, j, k \ \ln IM*} + \left(\mu_{\ln SAT_i, s, j, k (T_i) | \ln IM*} - \mu_{\ln SAT_i | \ln IM*} \right)^2 \right]}, \tag{13}$$

where $\sigma_{\ln SATi|\ln IM*}$ is the i-th element of the co-variance matrix and $p_{s,j,k}$ is the probability of the j-th scenario, k-th GMPE and s-th site, as it applies on the logarithmic mean value of the conditional spectral accelerations.

In order to illustrate the aforementioned approach for multi-site single-run CS record selection, a simple example is presented. We have assumed the M and R disaggregation results given in Table 1 for an IM level equal to 0.6g for six different sites. We have purposely considered an exaggerated difference between the most probable magnitude and distance ($\tilde{M}$ and $\tilde{R}$) points in the distribution of disaggregation results of the sites. These single most probable scenarios are used for CS computation for each site, neglecting the effect of multiple causal events for simplicity.

Table 1. The most probable *M*, *R* scenarios according to disaggregation, as assumed for six hypothetical sites.

Site #	S1	S2	S3	S4	S5	S6
$\tilde{R}$ (km)	10	10	30	30	50	50
$\tilde{M}$	6	7	6	7	6	7

DOI: XX

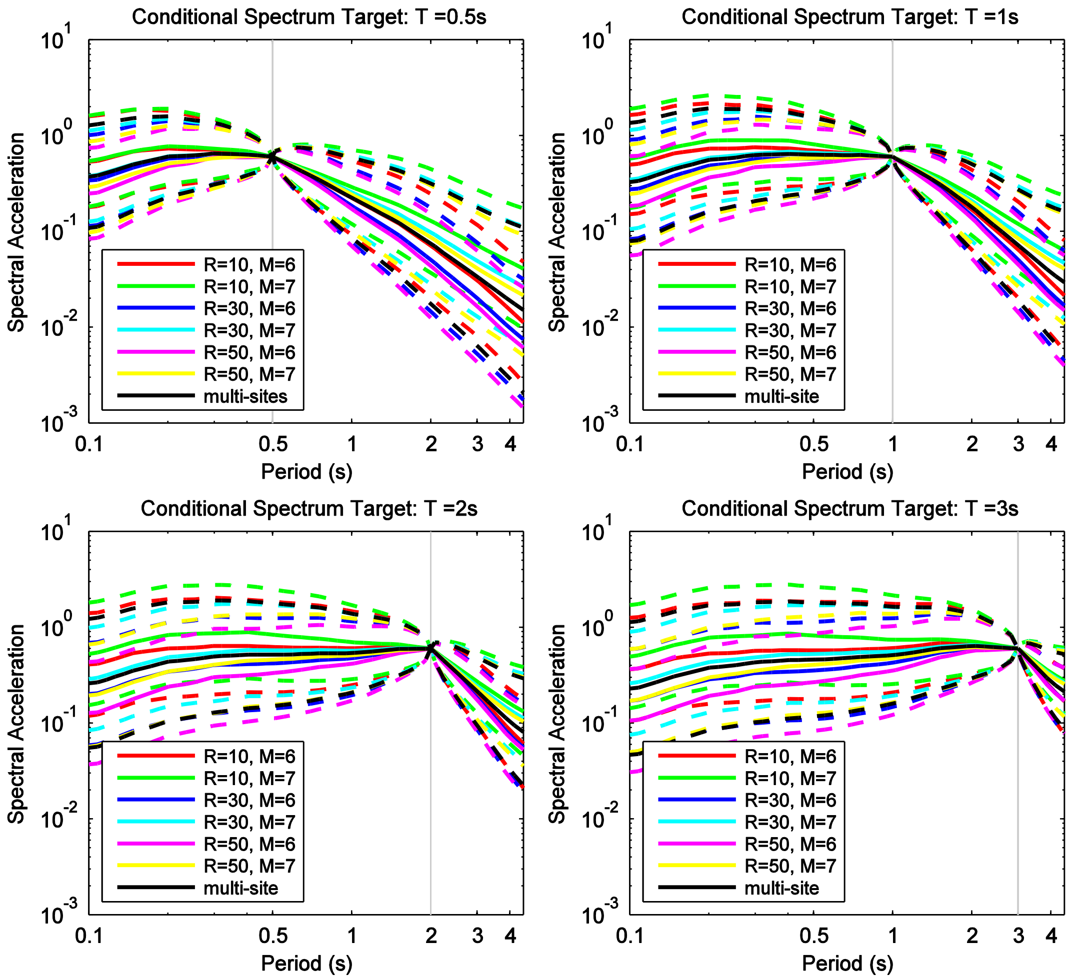

Figure 1. Target Conditional Spectra conditioned on *SAT* at six hypothetical sites with different "most contributing" scenarios. The black line is the CS target that incorporates all the sites. Solid lines indicate medians and dashed lines mark the 2.5th /97.5th percentiles.

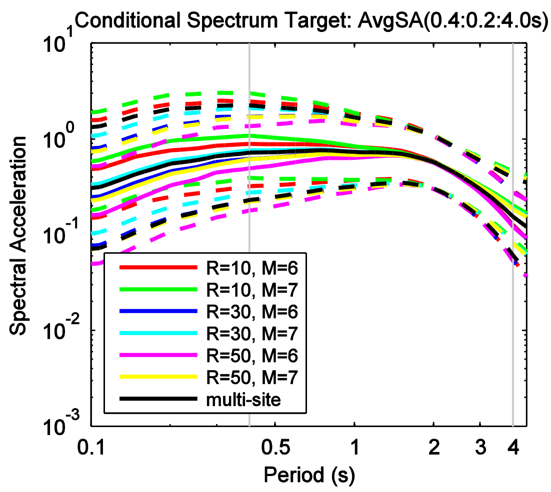

Figure 2. Target Conditional Spectra conditioned on *AvgSA* in a period range of 0.4:0.2:4.0s for the six hypothetical sites. The black lines represent the target CS incorporating all the sites. Solid lines indicate medians and dashed lines mark the 2.5th/97.5th percentiles.

DOI: XX

Figure 1 compares multiple target CS. They are conditioned on a given value of spectral acceleration at periods of 0.5, 1.0, 2.0 and 3.0s and for the most contributing scenarios for each of the six different sites. The black lines represent the CS targets where all sites were incorporated for use in the for the multi-site single-run fragility assessment. CS(*AvgSA*), in which *AvgSA* is defined in a period range of 0.4:0.2:4.0s is also adopted as a viable record selection target spectrum. The shorthand notation of 0.4:0.2:4.0s is used to denote a set of 18 periods ranging from 0.4s to 4.0s with an increment of 0.2s. The target CS(*AvgSA)* computed for all the scenarios corresponding to different sites appear in Figure 2. A visual comparison between Figure 1 and **Error! Reference source not found.** suggests that the scatter in the target spectrum when using *AvgSA* as conditioning IM, at least in the period range of interest, is lower than the scatter when *SAT* is used. In addition, *AvgSA* is well applicable to buildings with different fundamental periods, as it is defined over a range of periods rather than at a single one.

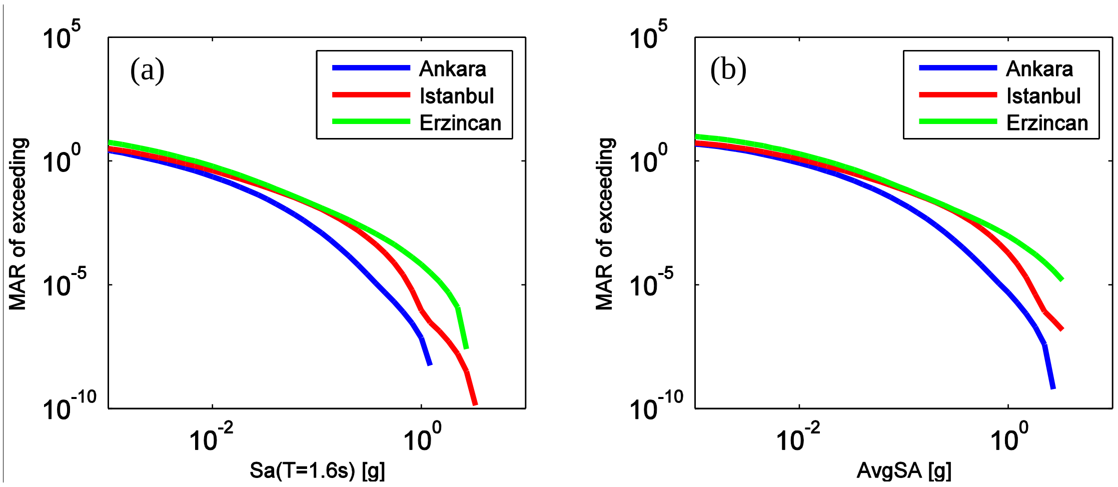

Figure 3. Hazard curves for Ankara, Istanbul and Erzincan for (a) *SA*(1.6s) and (b) *AvgSA* (0.4:0.2:4.0s).

4. CASE STUDY BUILDING EXAMPLES, SITES AND HAZARD

Four plan-symmetric moment-resisting frames are employed as case-studies, namely a 4-story steel frame, and three reinforced-concrete frames of 7, 12 and 20 stories. These are modern structures built to post-1980 seismic design provisions for high-seismicity regions (NEHRP site class D). A 2D centerline idealization of each building was modeled using OpenSees [58]. The behavior of the structural members was modeled by lumped-plasticity elements to increase speed of computation and to improve numerical convergence for large deformations. Geometric nonlinearities in the form of P-Δ effects were considered. Further details on the building properties and modeling approach appear in Kazantzi and Vamvatsikos [52]. The first modal periods of the buildings are 1.82, 1.60, 2.10 and 2.85s for the 4-, 7-, 12- and 20-story buildings, respectively.

We intend to derive fragility and vulnerability functions for three different sites with latitude and longitude of [32.76^o, 32.76^o], [28.96^o, 41.02^o] and [39.49^o, 39.74^o], representing the Turkish cities of Ankara, Istanbul and Erzincan, respectively. The OpenQuake [59], open-source software for seismic hazard and risk assessment developed by the Global Earthquake Model (GEM) Foundation was used to perform the seismic hazard computations. The analysis

DOI: XX

is based on the SHARE Project [60] source model and the GMPE proposed by Boore and Atkinson [61]. The hazard curves, showing the mean annual rate (MAR) of exceeding values of *SAT* at $T = 1.6$s and *AvgSA*(0.4:0.2:4.0s) for the three sites, appear in **Error! Reference source not found.**.

5. GROUND MOTION DATABASE

In order to show the site sensitivity of the global and local EDP response conditioned on the IM (and the corresponding fragility curves) of a given building model, multiple nonlinear dynamic analyses are performed according to the IDA [37] and MSA [38] paradigms. In IDA a fixed suite of ground motions is appropriately scaled to evaluate response at each IM level. Although MSA was originally cast to use a fixed record set, having little difference from IDA, we shall exploit instead the flexibility it allows to employ a different ground motion set at each IM level, selected each time according to the hazard of each site of interest. Of course, such flexibility comes at a price. Changing the conditioning IM in IDA is a simple, practical matter of post-processing. On the other hand, in MSA (as applied herein) changing the IM means reselecting the records and rerunning the structural analyses to maintain the benefit of hazard consistency.

The fixed IDA record set comprises the 22 pairs of motions of the FEMA P695 (ATC-63) [22] far-field ground motion set. These are strong ground motions originating from relatively large magnitude events appropriate for collapse prediction of modern structures. Record selection for MSA was performed at each IM level using two target spectra, namely CS(SAT_1) conditioned on the first mode of the vibration of each building, and CS(*AvgSA*) computed for the spectral ordinates at periods T = 0.4:0.2:4.0s. For each building, target spectrum and IM level, four record sets of equal size (44 accelerograms) were chosen. Three sets to match the hazard at each of the three sites, and the fourth record set to represent the hazard at all three sites together assuming equal weighting. We emphasize here that when *AvgSA* is adopted as the conditioning IM, a single period range may often be chosen to investigate the response of multiple buildings. This is the case herein, where the four buildings examined have fundamental periods T_1 = 1.6s – 2.85s. The period range of 0.4:0.2:4.0s used for *AvgSA* is meant to cover both the "elongation" of T_1 (say by a factor of about 1.5) due to damage and the periods shorter than T_1 corresponding to the higher modes affecting response. Thus, one does not need to differentiate among the different buildings when performing CS(*AvgSA*), significantly reducing the computational burden. For instance, for the period range of *AvgSA* defined in this study (i.e. 0.4:0.2:4.0s), most buildings with a first modal period of vibration within, say, 1.2 to 2.4s could be analyzed with considerable efficiency and sufficiency.

For both CS approaches, records from NGA-West ground motion database were selected and scaled to collectively match the entire distribution of the CS. To do so, we used the original algorithm developed for CS(*SAT*) [41] and its extended version for CS(*AvgSA*) [53]. For CS record sets, each consisting of 44 records, 10 IM levels were adopted, having fixed values of 0.01, 0.05, 0.08, 0.15, 0.25, 0.35, 0.50, 0.65, 0.80 and 0.95g to cover all ranges of the building response, from linear to nonlinear, until collapse. The target spectra were defined based on the mode (i.e., the most probable scenarios) of the M-R distributions from disaggregation results of the hazard. It is emphasized, however, that these 10 fixed IM levels, although used for both IM types, have different return periods when associated with different IMs. More specifically, they tend to correspond to higher hazard levels (longer return periods) for *AvgSA* than for SAT_1. Figure 4 shows the target spectra for CS(*SAT*) and CS(*AvgSA*) at IM level 5 for each individual site and for the multi-site approach together with the 44 individual

DOI: XX

records selected for the multi-site target. The median and 2.5th and 97.5th percentile spectra (or mean and 2.5th, 97.5th percentiles lines in log-space) of the FEMA P695 records used for IDA are also shown for comparison, scaled to SAT_1 and *AvgSA* corresponding to the IM level 5. This IM level (0.25g), for example, in Ankara corresponds to exceedance rates of 6.2×10^{-5} for SAT_1 at 1.6s and of 1.3×10^{-3} for *AvgSA*(0.4:0.2:4.0s).

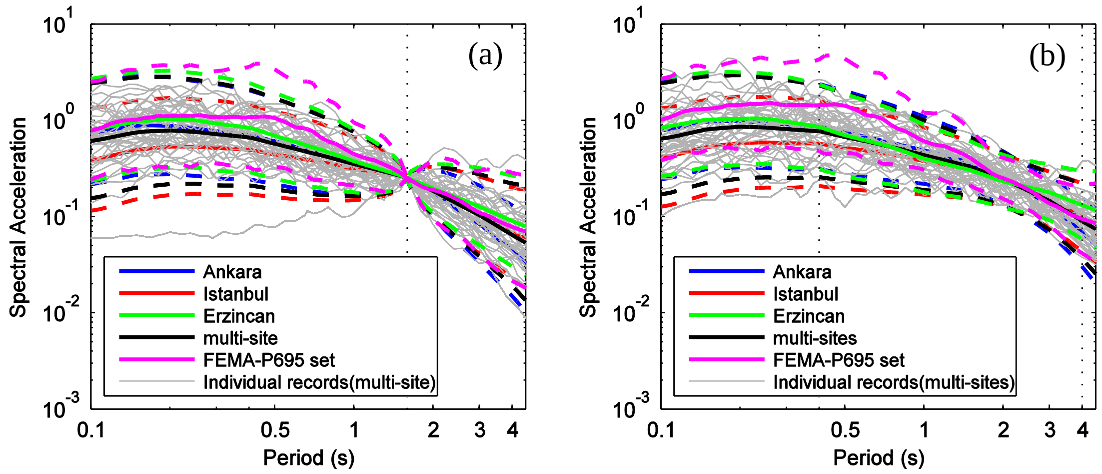

Figure 4. Record selection corresponding to the IM level 5 of 0.25g for the 7-story building for three sites using CS-based records versus the FEMA P-695 far-field set used for IDA: (a) CS(SAT_1), (b) CS(*AvgSA*). Thick solid lines indicate medians and dashed lines mark the 2.5th and 97.5th percentiles. The individual records shown in grey were selected via the multi-site single-run method.

6. ANALYSIS RESULTS

6.1. Local response of the building under different record selection schemes

The nonlinear dynamic analysis results based on IDA and MSA for the site of Ankara are shown in Figure 5. Figures 5(a) and (b) show the IDA curves corresponding to the maximum IDR along the height (MIDR) based on the conditioning IMs of SAT_1 and *AvgSA*, respectively. As can be seen, the dispersion in IDA when *AvgSA* is used as the conditioning IM is lower than that when SAT_1 is used instead. This suggests a higher efficiency of *AvgSA* compared to SAT_1, in line with the similar findings of previous studies (e.g. [45], [51]). Figure 5(c) and (d) display the MIDR response based on MSA and the conditioning IMs of SAT_1 and *AvgSA*, respectively. Each stripe consists of 44 data points related to the MIDR response, each one obtained from one nonlinear dynamic analysis. As was previously observed in Kohrangi et al. [53], the results obtained from the record set of CS(*AvgSA*) tend to maintain a uniform dispersion at different IM levels, which is a desirable feature, whereas the counterpart set of CS(SAT_1) produces less dispersed results for MIDR in the lower IM levels and more dispersed results at higher IM levels (i.e., at higher nonlinearity). This is because SAT_1 is naturally a better predictor for elastic response compared with *AvgSA* and it loses its efficiency at higher IM levels. *AvgSA*, on the other hand, is a moderately good IM at all IM levels from linear to nonlinear state of the structure (see [53] for more details). The MIDR results, however, present only a partial, although important, view about the building response. For a comprehensive loss assessment, an IM should predict an EDP well at different IM levels and at different locations within the building and also should perform well in estimating different EDP types, both acceleration- and displacement-based.

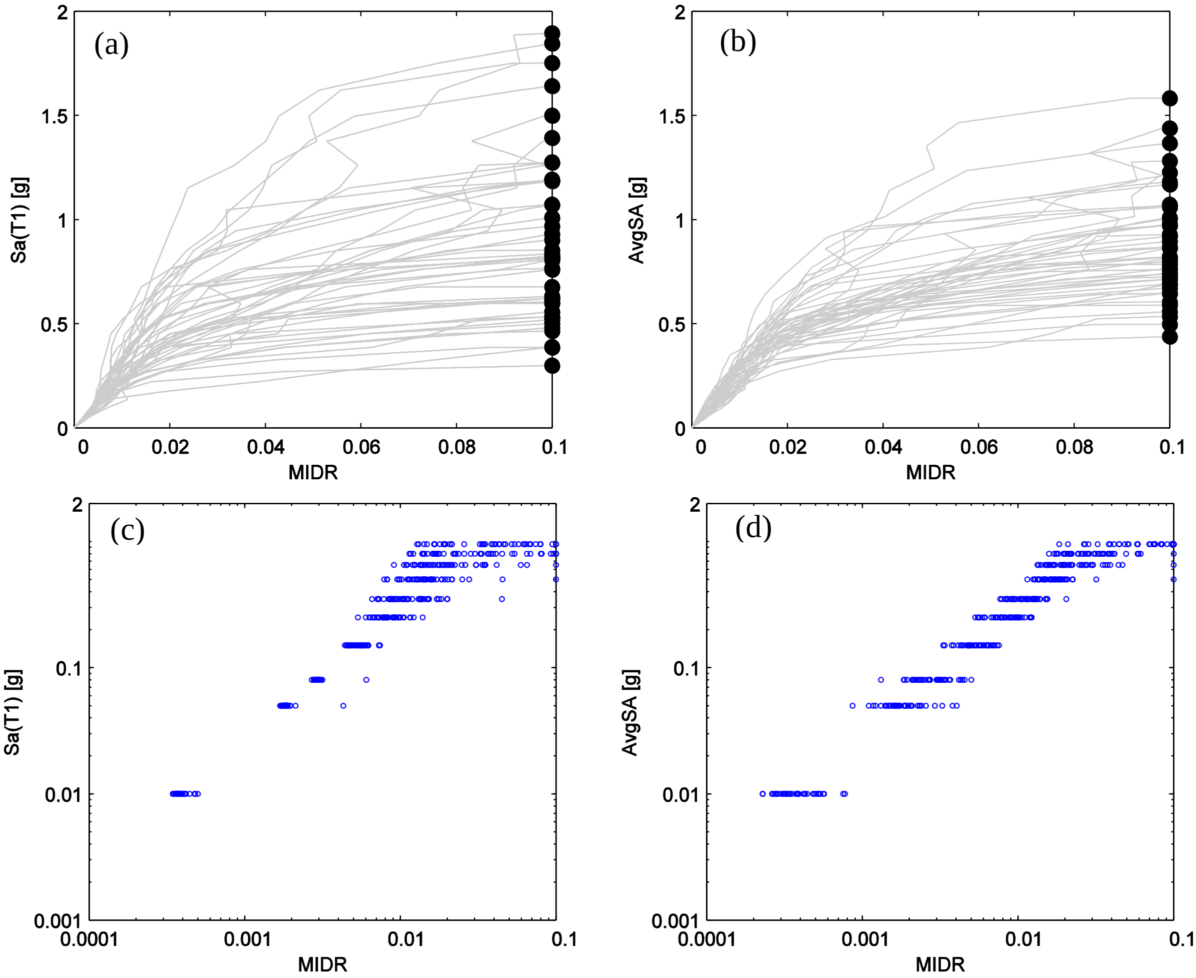

Figure 5. Nonlinear dynamic analysis results based on: IDA with (a) IM= SAT_1 and (b) IM=*AvgSA*, versus MSA with records selected for Ankara via (c) CS(SAT_1) and (d) CS(*AvgSA*).

Figure 6 shows the median IDR and PFA response profiles along the height of the 7-story frame obtained for the moderately intense IM level 6 of 0.35g from the records selected at different sites. The median response profile conditioned on SAT_1 appears in Figure 6 (a) and (b), while Figure 6 (c) and (d) show its counterpart conditioned on *AvgSA*. In both cases, the building response is significantly sensitive to the site hazard characteristics. For instance, for all the levels of IM (and not only the one shown here), the median response of the Erzincan building is higher than that of the buildings at all the other sites, while the building at Istanbul generally provides the lowest results. Furthermore, the site-sensitivity displayed obviously varies with the story and the type of EDP, e.g., appearing to be larger for the IDR of the top stories and the PFA of the lower floors. The fixed record set of IDA, on the other hand, by nature provides unique response estimates regardless of the site seismicity. In the case at hand, IDA highly overestimates the response in terms of both PFA and IDR. Interestingly, the adoption of *AvgSA* may bring the results of the different sites closer together, reducing the inter-site dispersion, yet at a first glance it seems to also increase the difference between IDA- and MSA-based results, something that would indicate reduced efficiency and sufficiency vis-à-vis SAT_1. However, care should be exercised here when visually comparing curves in different panels of the figure since, as mentioned earlier, comparing the responses at the same

DOI: XX

IM value here of 0.35g for *AvgSA* and SAT_1 actually means comparing responses with different likelihood of occurrence. This is because the occurrence of *AvgSA* equal to 0.35g is a rarer event (i.e., longer return period) than the occurrence of SAT_1 equal to 0.35g. This naturally translates to larger variability and larger differences in the median estimates of both MIDR and PFA.

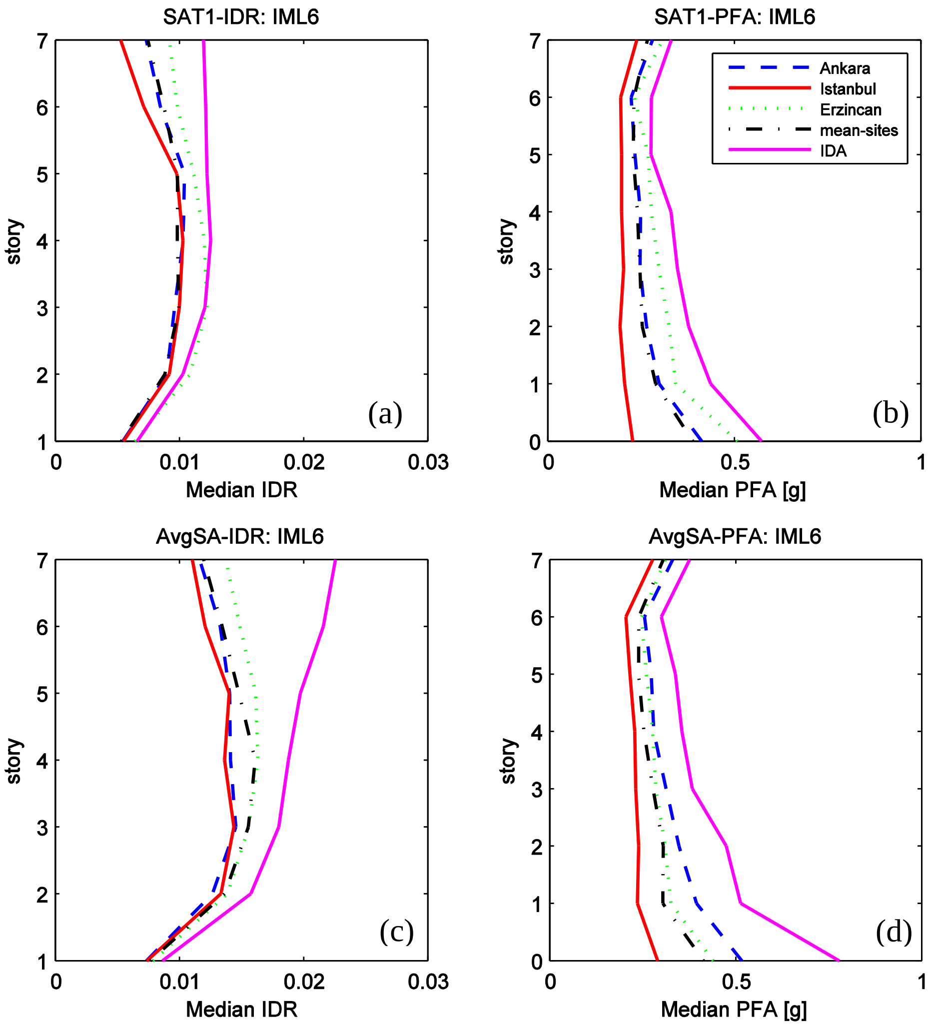

Figure 6. Building median IDR and PFA response profile of the 7-story building at different sites. The profiles were obtained at IM level 6 based on different record selections and two different conditioning IMs: (a) EDP=IDR and IM=SAT_1; (b) EDP=PFA, IM=SAT_1; (c) EDP=IDR, IM=*AvgSA*; (d) EDP=PFA, IM=*AvgSA*.

6.2. Analytical fragility functions

Several damage criteria have been proposed in the literature (see Akkar et al. [29], for instance), to assign buildings to a damage state and generate the corresponding fragility functions. These may be based on the maximum roof displacement, inter story drift ratio, steel or concrete strain level, maximum base shear, and so on. For illustrative purposes only and for the sake of simplicity, we have limited our consideration to only two EDPs: the maximum IDR along the building height (MIDR) as the damage measure gauging the overall structural performance up to global collapse, and the maximum PFA (MPFA) as indicative of floor accelerations occurring throughout the building. Actually, for comprehensive loss estimation according to component-based approaches [55], the ensemble of local IDRs and PFAs at each story are usually used, rather than the global MIDR and MPFA. Still, similar results (not shown here) have been obtained for local IDR and PFA at all stories and floors of each building examined.

For generating fragility curves based on MPFA and MIDR we selected four different Limit States, LS1 through LS4, ranging from low to extensive damage for each EDP type. For MIDR, the probability of exceeding drifts of 0.75, 1.2, 2.0 and 4.0% were assumed, whereas for MPFA the limit state thresholds were defined at acceleration values of 0.45, 0.55, 0.65 and 0.75g. Two of the resulting fragility curves obtained for MIDR and PFA are shown in Figure 7 and Figure 8, respectively. Therein, the site-specific fragility curves for the buildings in Ankara, Istanbul and Erzincan as well as the ones obtained from site-indifferent IDA are depicted. In addition, the fragility curves obtained using the proposed multi-site single-run methodology are compared against the arguably most accurate (and expensive) multi-run approach, using the weighted combination of site-specific fragility curves. For the example at hand, equal weighting of the sites has been adopted throughout. By inspecting Figures 7-8 we observe the following:

1. First and foremost, the building fragility functions are site-dependent, as was expected based on the results presented in the building analysis section. The difference in the fragility curves for different sites suggests that the common approach of applying a *single* fragility function can bring large uncertainty and bias into loss estimation unless the accelerograms used for its development are carefully selected to be consistent with the seismic hazard of the region. Thus, using one fragility curve for buildings located at multiple sites without appropriate consideration of the site-to-site hazard variability is not recommended when the seismicity of the region varies significantly. Nevertheless, this is essentially always the approach followed in practical applications where a single record set is compiled without rigorous record selection for the hazard characteristics of the sites and it is used to derive a single fragility/vulnerability curve for estimating the loss of all the like buildings in the region
2. The site-insensitive fixed record set used for IDA, in almost all cases, underestimates the building capacity. This might not be a general conclusion for every record set, since a main observation already is that different sets do produce different fragility curves. For instance, it seems that the FEMA P695 record set employed for IDA actually represents well the seismicity of the site of Erzincan for assessing MIDR, whereas it is far from representing well the seismicity of Ankara. However, in line with what was stated above one could conclude that using randomly selected record sets to perform dynamic analysis without at least some consideration to spectral shape and hazard consistency, can generate biased risk estimates. One might argue that the methodology introduced by Haselton et al. [35] may help to adjust the IDA results to achieve site-dependence. In that approach (adopted in FEMA P695 via a spectral shape factor), the median only (and not dispersion) of the fragility function obtained from IDA is adjusted based on the ratio between the mean of the epsilons of the records in the adopted set versus the expected mean epsilon of the records appropriate for the site (from hazard disaggregation) corresponding to a relevant hazard return period. Still, this method has been calibrated only for collapse assessment based on MIDR. It is not obvious whether such an approach could be applied successfully for predicting other limit-states based on either local or global EDPs.
3. The use of *AvgSA*, at least in the cases analyzed here, brings the fragility curves of buildings at different sites closer together compared to those obtained using SAT_1. This suggests that, even if the engineer decides to use a single fragility function for multiple-sites without performing careful record selection, developing it via IDA based on *AvgSA*

could be an acceptable approach. This feature of *AvgSA* could be explained with reference to its higher efficiency and sufficiency in building response prediction compared to SAT_1 [52, 53]. On the other hand, even in cases where SAT_1 is adequately sufficient (e.g., low-to-moderate ductility first-mode dominated buildings), one would have to employ a single common period to be able to combine the resulting fragility/vulnerability curves from different buildings. Even if one were to employ CS(SAT_1) to further correct for insufficiency, the subsequent change to a different (common) period would probably nullify most benefits, as the convolution with the hazard would not involve T_1 anymore. Using *AvgSA* instead of SAT_1 as the IM is actually the simplest suggestion that would painlessly improve the fidelity of the current state of practice before introducing the benefits of CS record selection.

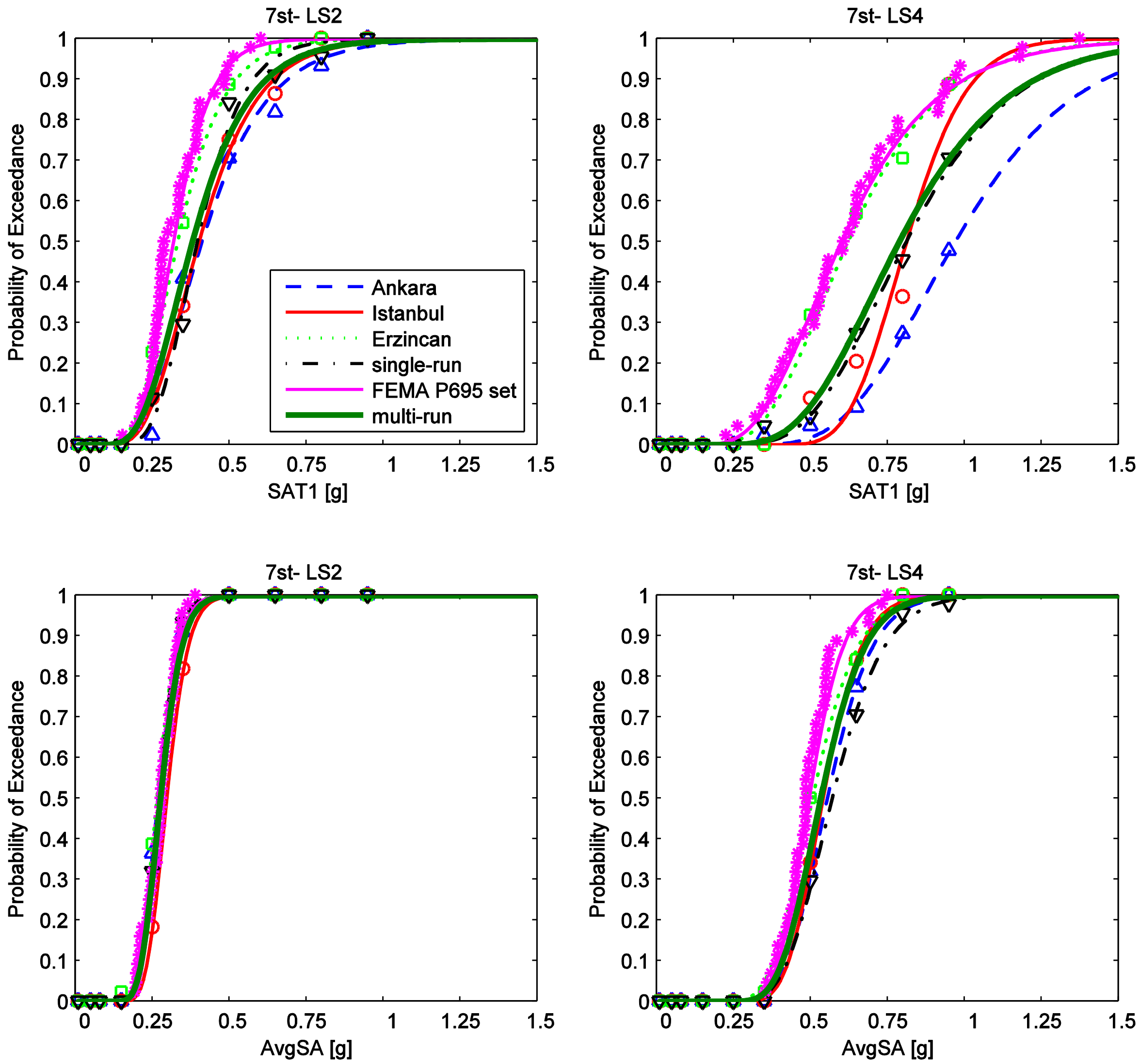

Figure 7. MIDR fragility curves obtained for two limit-states of the 7-story building based on SAT_1 and *AvgSA* and on record sets selected for different sites. Limit-states LS2 (left) and LS4 (right) are defined for MIDR values exceeding 1.2% and 4.0%, respectively.

DOI: XX

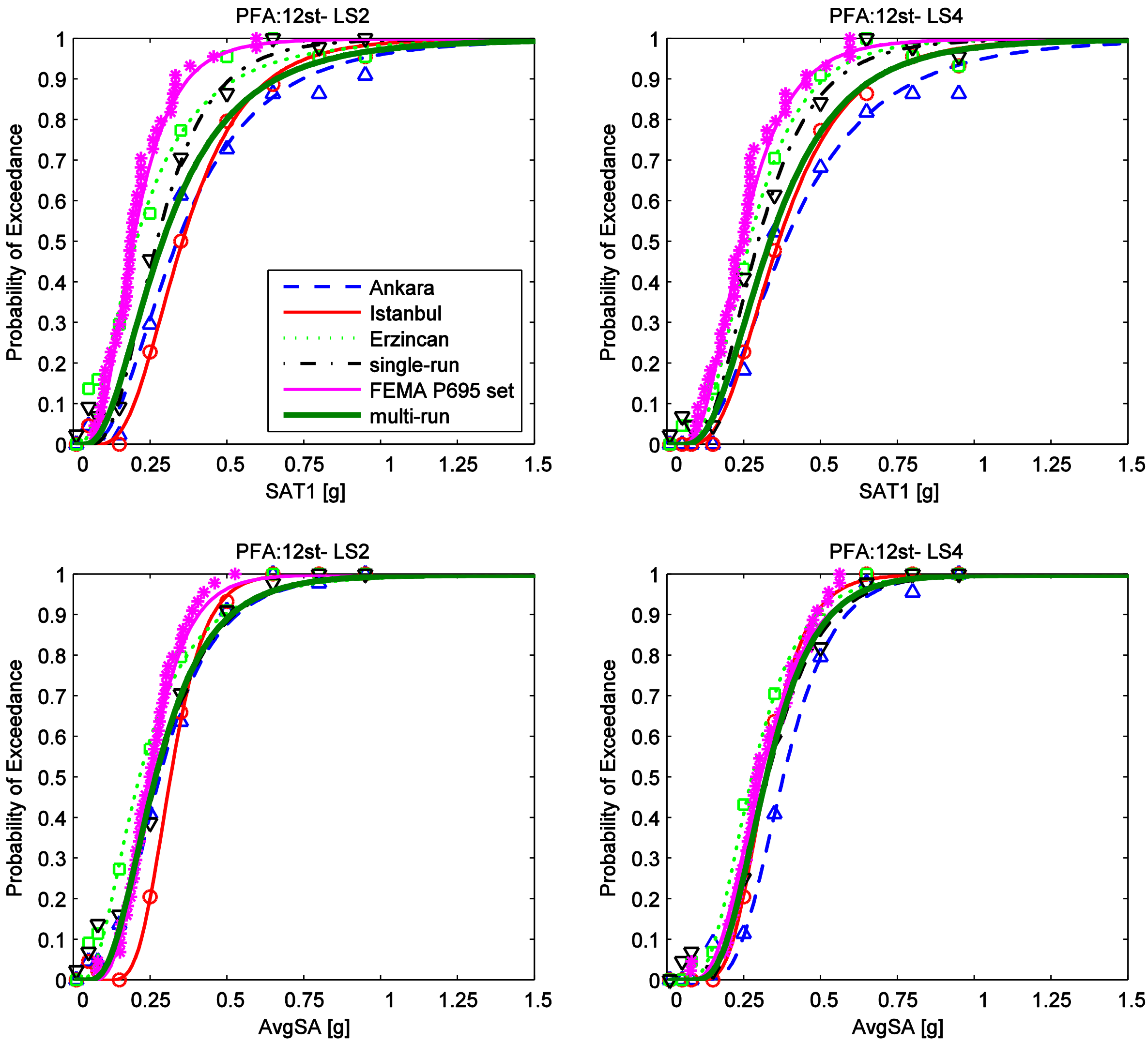

Figure 8. MPFA fragility curves obtained for two limit-states of the 12-story building based on SAT_1 and *AvgSA* and on record sets selected for different sites. Limit-states LS2 (left) and LS4 (right) are defined for MPFA values exceeding 0.55g and 0.75g, respectively.

4. The proposed single-run multi-site methodology provides results that are very close to the comprehensive multi-run multi-site approach used as a benchmark. Whenever one fragility curve is sought to represent buildings at multiple sites, both methods offer a result that incorporates the input of all sites according to the assigned weights and sits in between their individually estimated fragility functions. Yet, the single-run approach does so at a vastly reduced cost, requiring exactly $1/N$ of the dynamic analyses per archetype building when N sites are involved. Of course, the question still remains whether one fragility (per limit-state) or vulnerability, no matter how carefully crafted, can be used to accurately estimate the regional loss for a class of buildings. Yet, for purely practical reasons, this is the approach that is universally adopted. Only future research can provide a definitive answer.

6.3. Vulnerability functions

There are two main approaches to obtaining analytical vulnerability functions, namely the component-based and the building-based [20]. The former employs component-fragility functions (i.e., probability functions of the EDP) to assign damage and estimate losses at the level of each structural/non-structural/content component separately. The latter employs building-fragility functions (i.e., the probability functions of the selected IM) for different limit states to assess structural/non-structural/content damage at the level of the entire building. Then, consequence functions (i.e., relationships between limit states and expected losses usually expressed as a fraction of the building replacement cost) are used to provide the link between building damage and loss. The consequence functions are usually obtained by expert judgment or are based on empirical damage and loss data from past earthquakes; one could also obtain them through building-specific loss estimation process [12]. In other words, the combination of fragility and consequence functions generates a vulnerability function (e.g., mean loss ratio and corresponding coefficient of variation as a function of the selected IM).

As an example, to develop a vulnerability function for these buildings we shall employ the building-level approach using the consequence functions introduced by Bal et al. [62] for Turkish buildings. Therein, the (mean) loss ratios are defined as 0.10, 0.3, 0.6 and 1.0 corresponding to slight, moderate, extensive and near-collapse limit states. The MIDR-based fragilities derived earlier using drift thresholds of 0.75, 1.2, 2.0 and 4.0% are now employed to define the onset of the four limit-states of interest. The results obtained for the 7-story building are shown in Figure 9. As expected, the vulnerability functions obtained when using *AvgSA* are much closer and considerably less spread compared to the same curves obtained using SAT_1. A more comprehensive component-based estimation using local EDPs may have shown a larger sensitivity to the site, yet the summation operation inherent in loss aggregation tends to average out some of the differences. Yet, as Figure 9 shows, this is not enough to fully erase site-dependence even when *AvgSA* is employed. Either way, the proposed single-run approach offers practically identical results to the expensive multi-run baseline, offering a good way to incorporate the effect of different sites without computational waste.

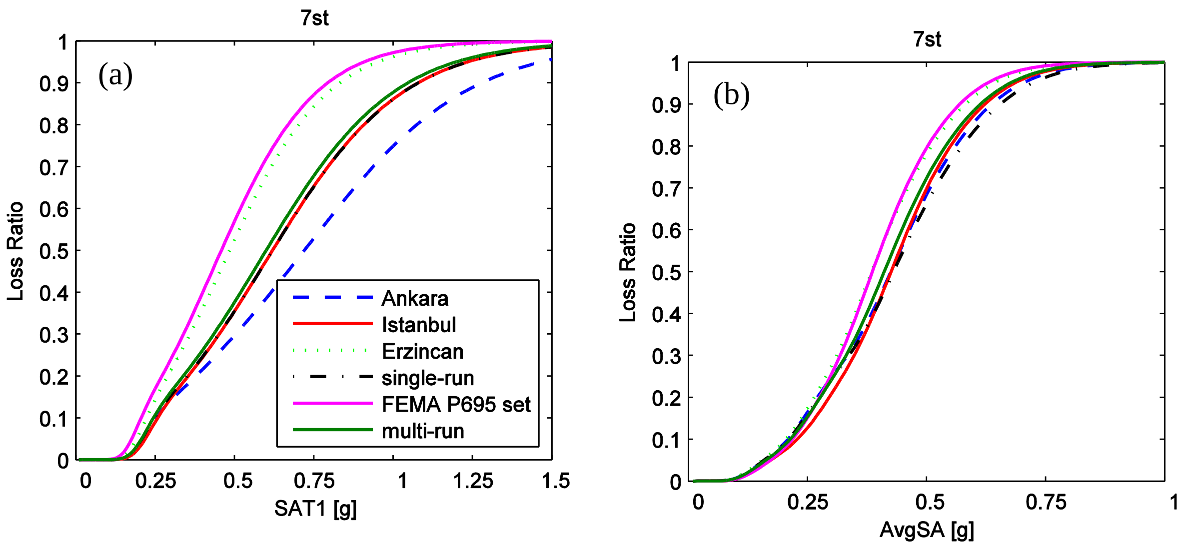

Figure 9 Mean loss ratio vulnerability functions obtained for the 7-story building hypothetically located in Ankara, Istanbul, and Erzincan.

DOI: XX

7. DISCUSSION

The results presented support the application of advanced IMs (e.g. *AvgSA*) in portfolio loss estimations. It should be emphasized that, despite the existence of other IMs in the literature that might have similar benefits to *AvgSA*, since hazard computations for *AvgSA* (or any other geometric mean of logarithms of spectral ordinates) can be based on the available GMPEs and PSHA codes [53], its application is considerably more appealing. The use of *AvgSA* also allows for smaller scaling factors in the CS method than those necessary when utilizing SAT_1 [53]. This is especially important when trying to predict the collapse capacity of modern buildings, as some ground motion scaling is nearly always needed. Using a relatively small scaling factor while maintaining hazard consistency assures higher fidelity.

In both methodologies introduced to combine multiple sites (single- and multi-run), the user can provide appropriate weights when incorporating the sites into a single record set (single-run) or a single fragility function (multi-run). For the case study presented, even though the seismicity of Erzincan is higher than that of Istanbul or Ankara, in any portfolio of practical interest there are probably more buildings of any given class in the latter two cities than in Erzincan. Thus, in a real application one could opt to give Istanbul and Ankara more weight (e.g., equal to the fraction of the building portfolio in each city) to provide a better compromise for the single fragility/vulnerability curve provided by the multi-run or the single-run options.

Both multi-site approaches offered employ a single fragility curve for all the sites considered in the loss assessment procedure. Such a fragility curve is based on the *law of total variability* via Equations (4) or (13) and will incorporate higher total dispersion compared to each of the fragilities obtained for a single site. This higher dispersion will be translated to somewhat higher loss estimates due to the larger tails in the distribution. This is a natural consequence of such an approximation. At the same time this is computationally more efficient than estimating multiple site-dependent fragility curves, and more accurate than the current practice of a single site-independent fragility. It obviously represents a trade-off between speed and accuracy to be evaluated by the analyst for each case at hand. Nonetheless, the results show that any increase in the variability could be significantly reduced using *AvgSA* as the conditioning IM, thanks to its higher efficiency and sufficiency that brings the fragilities of different sites closer to each other (see Figures 7 and 8).

One issue that may become problematic for regional loss estimation is that different sites with significantly different tectonic settings (such as crustal versus subduction interface) may also require consideration of other ground motion characteristics beyond spectral shape, such as duration or near source pulses. In such cases one may need to take into account the distribution of such characteristics, e.g., via GCIM [42]. Nevertheless, duration-sensitive metrics are mainly important for limit-states near global collapse [63]. For losses, though, which are typically dominated by lower limit-states, duration parameters may not be as significant.

8. CONCLUSIONS

We proposed two methods to incorporate the effect of multiple sites in the estimation of ensemble fragility and vulnerability studies. The conceptually simpler and computationally more expensive approach involves carrying out record selection at each site, performing analysis to obtain the corresponding fragility/vulnerability, and combining them into a single function to be used at all sites. A more subtle and elegant approach involves incorporating the site effect directly into the record selection. In practice, this translates into selecting a single record set per IM utilized for assessing the building response and thus needing the same (low) number of dynamic analyses regardless of the number of sites considered.

In addition, we examined two different IMs based on spectral acceleration ordinates: the spectral acceleration at the first mode of vibration, SAT_1, and the geometric mean of spectral acceleration over a period range, *AvgSA*. The results show that when *AvgSA* is used, the scatter in the response of identical buildings located at different sites is greatly diminished in comparison to when SAT_1 is utilized. The use of *AvgSA* in fact considerably reduces the effect of the different ground motions characteristics expected at different sites on the predicted response. Thus, whenever rigorous record selection is not used, *AvgSA* can still be employed to lessen the negative impact of this omission. Additional advantages of *AvgSA*, such as its efficiency in global and local response prediction as well as its potential for serving as a single common IM for a class of buildings, make it an ideal yet practical solution for portfolio loss and risk assessment. Obviously, many important challenges still remain. Soft-soil amplification, near-source directivity and ground motion duration may influence the site-specific response of any building, introducing significant difficulties in the generation of fragility or vulnerability function with wide coverage. Still, it may be convincingly argued that the issue of spectral shape can be comprehensively handled within the proposed framework. Even though further validation is needed to fully map the potential of such approaches, they are arguably far more advanced than all current site-indifferent techniques for developing fragility/vulnerability functions.

ACKNOWLEDGEMENTS

Financial support for the first author provided by “Iranian National Elites Foundation” is greatly acknowledged.

9. REFERENCES

1. Kircher CA, Reitherman RK, Whitman RV, Arnold C. Estimation of Earthquake Losses to Buildings. *Earthquake Spectra* 1997; **13**(4): 703−720.
2. Orsini G. A Model for Buildings’ Vulnerability Assessment Using the Parameterless Scale of Seismic Intensity (PSI). *Earthquake Spectra* 1999; **15**(3): 463−483.
3. Rossetto T, Elnashai A. Derivation of Vulnerability Functions for European-Type RC Structures Based on Observational Data. *Engineering Structures* 2003. **25**(10): 1241−1263.
4. Di Pasquale G, Orsini G and Romeo RW. New Developments in Seismic Risk Assessment in Italy. *Bulletin of Earthquake Engineering* 2005; **3**(1): 101−128.
5. Porter KA, Kennedy RP, and Bachman RE. Creating fragility functions for performance-based earthquake engineering. *Earthquake Spectra* 2007; **23**(2): 471–489.
6. Straub D, Der Kiureghian A. Improved seismic fragility modeling from empirical data. *Structural Safety* 2008; **30**(4): 320–336.
7. Rossetto T, Ioannou I, Grant DNE. Existing empirical fragility and vulnerability functions: Compendium and guide for selection 2013; GEM Technical Report, GEM Foundation, Pavia, Italy.
8. Rossetto T, Ioannou I, Grant DN, Maqsood T. Guidelines for Empirical Vulnerability Assessment, 2014, GEM Technical Report, GEM Foundation, Pavia.
9. Noh HY, Lallemant D, Kiremidjian AS., Development of empirical and analytical fragility functions using kernel smoothing methods. *Earthquake Engineering and Structural Dynamics* 2015; **44**: 1163–1180.

10. Kennedy RP, Ravindra MK. Seismic fragilities for nuclear power plant risk studies. *Engineering and Design* 1984. **79**(1): 47–68.
11. Park YJ, Ang AH. Mechanistic Seismic Damage Model for Reinforced Concrete. *Journal of Structural Engineering* 1985; **111**(4): 722–739.
12. Porter K, Farokhnia K, Vamvatsikos D, Cho IH. Guidelines for component-based analytical vulnerability assessment of buildings and nonstructural elements, 2014, Global Earthquake Model Foundation, Pavia, Italy: GEM Technical Report 2014-13.
13. Whitman RV, Anagnos T, Kircher, CA, Lagorio HJ, Lawson, Schneider P. Development of a National Earthquake Loss Estimation Methodology. *Earthquake Spectra* 1997; **13**(4): 643–661.
14. FEMA, HAZUS99 Technical Manual, in Federal Emergency Management Agency1999: Washington, DC, U.S.A.
15. FEMA, HAZUS99 Estimated Annualized Earthquake Loss for the United States, in Federal Emergency Management Agency, R.F. 366, Editor 2001: Washington, DC, U.S.A.
16. Masi A. Seismic Vulnerability Assessment of Gravity Load Designed R/C Frames. *Bulletin of Earthquake Engineering and Design* 2003; **1**(3): 371–395.
17. FEMA, HAZUS-MH Technical Manual, F.E.M. Agency, Editor 2003: Washington, DC, U.S.A.
18. Rossetto T, Elnashai A. A New Analytical Procedure for the Derivation of Displacement-Based Vulnerability Curves for Populations of RC Structures. *Engineering Structures* 2005; **7**(3): 397–409.
19. Silva V, Crowley H, Varum H, Pinho R, Sousa R. Evaluation of analytical methodologies used to derive vulnerability functions. *Earthquake Engineering and Structral Dynamics* 2014. **43**:181–204.
20. D'Ayala D, Meslem A, Vamvatsikos D, Porter K, Rossetto T. Guidelines for Analytical Vulnerability Assessment of Low/Mid-Rise Buildings 2014; Global Earthquake Model Foundation, Pavia, Italy. GEM Technical Report 2014-12.
21. Silva V, Crowley H, Varum H, Pinho R, Sousa, R. Investigation of the characteristics of Portuguese regular moment-frame RC buildings and development of a vulnerability model. *Bull Earthquake Engineering* 2014.
22. FEMA. Quantification of building seismic performance factors, FEMA P695. Applied Technology Council for the Federal Emergency Management Agency, Washington, DC, 2009.
23. Reitherman R, Cobeen K. Design documentation of woodframe project index buildings. Publication W-29, Consortium of Universities for Research in Earthquake Engineering, Richmond, CA, 2003.
24. ATC, Earthquake Damage Evaluation Data for California, in Applied Technology Council, R. ATC-13 1985: Redwood City, California, U.S.A.
25. Brzev S, Scawthorn C, Charleson AW, Allen L, Greene M, Jaiswal K, Silva V. GEM Technical Report 2013-02; GEM Foundation, Pavia, Italy.
26. Kappos AJ, Pitilakis K, Stylianidis KC. Cost-Benefit Analysis for the Seismic Rehabilitation of Buildings in Thessaloniki, Based on a Hybrid Method of Vulnerability Assessment. Fifth International Conference on Seismic Zonation. 1995. Nice, France.
27. Kappos AJ, Stylianidis KC, Pitilakis K. Development of Seismic Risk Scenarios Based on a Hybrid Method of Vulnerability Assessment. *Natural Hazards* 1998. **17**(2): 177–192.
28. Barbat AH, Yépez Moya F, Canas, JA. Damage Scenarios Simulation for Seismic Risk Assessment in Urban Zones. *Earthquake Spectra* 1996. **12**(3): 371–394.
29. Akkar S, Sucuoglu H,Yakut A. Displacement-based fragility functions for low- and mid-rise ordinary concrete buildings. *Earthquake Spectra* 2005; **21**(4): 901–927.
30. Bommer JJ, Crowley H. The influence of ground-motion variability in earthquake loss modelling. *Bulletin of Earthquake Engineering* 2006; **4**(3):231–248.
31. Sousa ML, Campos Costa A, Carvalho A, Coelho E. An Automatic Seismic Scenario Loss Methodology Integrated on a Geographic Information System. In Proceedings of the 13th World Conference on Earthquake Engineering. 2004. Vancouver, Canada: Paper No. 2526 (on CD).
32. Calvi GM, Pinho R (2004). LESSLOSS – A European integrated project on risk mitigation for earthquakes and landslides, Research Report Rose 2004/02, Pavia, Italy.

DOI: XX

33. Pinho R, Bommer JJ, Glaister S. A Simplified Approach to Displacement-Based Earthquake Loss Estimation Analysis. in Proceedings of the 12th European Conference on Earthquake Engineering. 2002. London, U.K.: Paper No. 738 (on CD).
34. Restrepo-Velez, Luis F, Magenes, G. Simplified procedure for the seismic risk assessment of unreinforced masonry buildings. In Proceedings of the 13th World Conference on Earthquake Engineering. 2004, Vancouver, Canada.
35. Haselton C, Baker J, Liel A, Deierlein G. Accounting for ground-motion spectral shape characteristics in structural collapse assessment through an adjustment for epsilon. *Structural Engineering* 2011; **137**(3): 332–344.
36. Jayaram N, Shome N, Rahnama M. Development of earthquake vunerability functions for tall buildings. *Earthquake Engineering and Structural Dynamics* 2012; **41**: 1495–1514.
37. Vamvatsikos D, Cornell CA. Incremental dynamic analysis. *Earthquake Engngineering and Structural Dynamics* 2002. **31**(3): 491–514.
38. Jalayer F. Direct Probabilistic Seismic Analysis: Implementing Non-linear Dynamic Assessment, in Department of Civil and Environmental Engineering2003, Stanford University: Stanford, CA.
39. Luco N, Cornell CA. Structure-Specific Scalar Intensity Measures for Near-Source and Ordinary Earthquake Ground Motions. *Earthquake Spectra* 2007; **23**(2): 357–392.
40. Baker JW. The conditional mean spectrum: A tool for ground motion selection. *ASCE Journal of Structural Engineering* 2011; **137**: 322–331.
41. Jayaram N, Lin T, Baker JW. A Computationally Efficient Ground-Motion Selection Algorithm for Matching a Target Response Spectrum Mean and Variance. *Earthquake Spectra* 2011. **27**(3): 797–815.
42. Bradley BA. A generalized conditional intensity measure approach and holistic ground-motion selection. *Earthquake Engineering and Structural Dynamics* 2010; **39**(12): 1321–1342.
43. Porter K, Farokhnia K, Vamvatsikos D Cho IH. Guidelines for component-based analytical vulnerability assessment of buildings and nonstructural elements. *GEM Technical Report 2014-13,* Global Earthquake Model Foundation, Pavia, Italy, 2014. DOI: 10.13117/GEM.VULN-MOD.TR2014.13.
44. Baker JW, Cornell CA. Spectral shape, epsilon and record selection. *Earthquake engineering and structural dynamics* 2006. **35**(9): 1077–1095.
45. Cordova PP, Deierlein GG, Mehanny SS, Cornell CA. Development of a two-parameter seismic intensity measure and probabilistic assessment procedure. in 2nd US–Japan Workshop on Performance-based Earthquake Engineering Methodology for RC Building Structures, Sapporo, Hokkaido, 2000.
46. Bianchini M, Diotallevi P, Baker JW. Prediction of Inelastic Structural Response Using an Average of Spectral Accelerations, in 10th International Conference on Structural Safety and Reliability (ICOSSAR09)2010: Osaka, Japan.
47. Vamvatsikos D, Cornell CA. Developing efficient scalar and vector intensity measures for IDA capacity estimation by incorporating elastic spectral shape information. *Earthquake Engineering and Structural Dynamics* 2005. **34**: 1573–1600.
48. Bojórquez E, Iervolino I, Spectral shape proxies and nonlinear structural response. *Soil Dynamics and Earthquake Engineering* 2011; **31**(7): 996–1008.
49. Bradley BA. Site-Specific and Spatially Distributed Ground-Motion Prediction of Acceleration Spectrum Intensity. *Bulletin of the Seismological Society of America* 2010; **100**: 792–801.
50. Bradley BA. Empirical equations for the prediction of displacement spectrum intensity and its correlation with other intensity measures. *Soil Dynamics and Earthquake Engineering* 2011; **31**: 1182–1191.
51. Eads L, Miranda E, Lignos, DG. Average spectral acceleration as an intensity measure for collapse risk assessment. *Earthquake Engineering and Structural Dynamics* 2015; **44**(12), 2057–2073.
52. Kazantzi AK, Vamvatsikos D. Intensity measure selection for vulnerability studies of building classes. *Earthquake Engineering and Structural Dynamics* 2015; **44** (15), 2677–2694.
53. Kohrangi M, Bazzurro P, Vamvatsikos D, Spillatura A. Conditional Spectrum-based ground motion selection using average spectral acceleration. *Earthquake Engineering and Structural*

Dynamics 2015 (Under review).
54. Lin T, Harmsen SC, Baker JW, Luco N. Conditional spectrum computation incorporating multiple causal earthquakes and ground motion prediction models. *Bulletin of the Seismological Society of America* 2013; 103(2A): 1103–1116.
55. FEMA, Seismic Performance Assessment of Buildings, FEMA P-58-1. Applied Technology Council for the Federal Emergency Management Agency, 2012.
56. Baker JW. Efficient analytical fragility function fitting using dynamic structural analysis. *Earthquake Spectra* 2015; **31**(1): 579–599.
57. Weiss NA, A Course in Probability. Addison–Wesley. 2005.
58. McKenna F, Fenves G, Jeremic B, Scott M. Open system for earthquake engineering simulation. <http://opensees.berkeley.edu> (Jan 2014), 2000.
59. Monelli D, Pagani M, Weatherill G, Silva V, Crowley H. The hazard component of OpenQuake: The calculation engine of the Global Earthquake Model. in 15th World Conference on Earthquake Engineering, Lisbon, Portugal. 2012.
60. Giardini D, et al. Seismic Hazard Harmonization in Europe (SHARE). Online data resource, Swiss Seismological Service, 2013: p. ETH Zurich, Zurich, Switzerland, [Available at: http://www.efehr.org:8080/jetspeed/].
61. Boore DM, Atkinson GM. Ground-Motion Prediction Equations for the Average Horizontal Component of PGA, PGV, and 5%-Damped PSA at Spectral Periods between 0.01 s and 10.0 s. *Earthquake Spectra* 2008; **24**(1): 99–138.
62. Bal IE, Crowley H, Pinho R, Gulay F. Detailed assessment of structural characteristics of Turkish RC building stock for loss assessment models. *Soil dynamics and earthquake engineering* 2008; **28**: 914–932.
63. Raghunandan M, Liel AB. Effect of ground motion duration on earthquake-induced structural collapse. *Structural Safety* 2013; **41**: 119–133.

DOI: XX